

Stress and magnetic field dependent Young's modulus in single crystal iron-gallium alloys

S. Datta ^{1*}, J. Atulasimha ², C. Mudivarthi ³ and A. B. Flatau ^{1,3}

¹ 3181 Martin Hall, Department of Aerospace Engineering, University of Maryland, College Park, MD 20742, USA,
Phone: +1-301-405-2002, Fax: +1-301-314-9001, Email: supratik@umd.edu

² Department of Mechanical Engineering, Virginia Commonwealth University, Richmond, VA 23284, USA

³ Department of Materials Science and Engineering, University of Maryland, College Park, MD 20742, USA

ABSTRACT

Magnetostrictive materials exhibit an apparent change in Young's modulus at different magnetization and stress states. In this work, the variability in modulus is investigated using experiments and simulations of single crystal iron-gallium (Galfenol) alloys having 16 and 19 atomic percent gallium. Both of these alloys showed more than 60 % change in Young's modulus along [100] direction on varying their magnetization and stress states compared to their modulus at saturation state. A review of methods for quantifying variability in modulus is provided and for use in device design, a function, $\Delta E(\sigma, H)$, is introduced for bounding variability of modulus between 0 and 100 %. An energy-based non-linear constitutive model was used to predict the variable modulus in Galfenol as a continuous function of stress and magnetic field. Model predictions show good correlation with experimental results. The ability to model and quantify the variation in modulus provides tools for design of smart material applications where the ability to vary and control modulus is of interest.

Keywords: Magnetostriction, ΔE effect, $\Delta E(\sigma, H)$, Magnetoelastic, Young's modulus, Iron-gallium alloys (Galfenol)

1. INTRODUCTION

Magnetostrictive materials exhibit an apparent change in Young's modulus at different magnetization and stress states [1]. Hence, the Young's modulus in magnetostrictive materials under a particular stress can be controlled in real time by changing magnetic field (H), which can be useful in various applications such as tunable resonator [2], active vibration control [3], impedance matching in magnetostrictive actuation and controlling acoustic wave propagation.

The apparent change in Young's modulus owes its origin to the magnetomechanical coupling present in magnetostrictive materials. The total strain (ε) in such materials is obtained by the superposition of elastic and magnetoelastic strains as shown in Eq. (1).

$$\varepsilon(\sigma, H) = \frac{\sigma}{E_s} + \lambda(\sigma, H) \quad (1)$$

While the elastic strain is only dependent on the mechanical stress (σ) and a purely

mechanical Young's modulus (E_S) of the material, the magnetoelastic strain (λ) arises due to both stress and magnetic field. A magnetic field or stress applied to the material changes the alignment of the atomic magnetic moments in the material which is often manifested as a change in magnetization and magnetoelastic strain in the material. The magnetoelastic strain adds to the elastic strain until the material is saturated, beyond which only elastic strain occurs.

There are two kinds of saturation in magnetostrictive material – magnetic and magnetoelastic. Application of a magnetic field high enough to overcome both a pre-stress imposed on the material and the material's magnetocrystalline anisotropy (K) can cause magnetic saturation of the material by aligning all the magnetic moments parallel to the direction of magnetic field. Application of tensile or compressive stresses high enough to overcome a bias magnetic field and the magnetocrystalline anisotropy can magnetoelastically saturate the material by aligning all the magnetic moments antiparallely. At high tensile stresses, the magnetic moments align at 0° and 180° from the direction of stress whereas at high compressive stresses, the magnetic moments align at 90° and 270° from the direction of stress. It is this reorientation of the magnetic moments which manifests as an apparent change in Young's modulus.

Young's modulus, which is defined as the ratio of incremental change in applied stress to that of incremental change in total strain, appears to be softer than a purely mechanical Young's modulus when the magnetoelastic strain varies with stress and magnetic field in an unsaturated sample. Once the material saturates and the magnetoelastic strain becomes a constant, the value of Young's modulus asymptotes towards a constant. This constant value is called by various names such as stiff/hard modulus, Young's modulus at saturation (E_S) and as a purely mechanical Young's modulus.

Early work [1] based on tensile testing of iron/nickel alloy wires used the term ΔE effect at a constant stress as $(E_H - E_a)/E_H$. Here E_a is the modulus of the material at demagnetized state and is also known as the soft modulus while E_H is the modulus at an applied magnetic field H . The modulus was calculated by applying different constant stresses to the wires and measuring the strains due to an incremental change in stress under demagnetized state and different applied magnetic fields respectively. Both positive and negative values of ΔE effect were shown and the highest ΔE effect of 25.2 % was observed in 70.32 % Nickel-Steel at a stress of 16 MPa and an applied field of 0.76 kA/m. In a separate work [4], a linearly decreasing strain-dependent modulus ($E^{-1}dE/d\varepsilon \sim 5 \times 10^{-6}$) was observed in nickel alloys.

Assuming a purely rotational magnetization process, the first analytical expression for the ΔE effect was derived by Becker and Doring [5]. Lee [6] reported a mathematical interpretation of the ΔE effect and reviewed contemporary works to point out that since E_a depends on the magnetocrystalline anisotropy (K) of the material, a material with higher K should exhibit a smaller ΔE effect. Although it was shown that the Young's modulus in a demagnetized state depends on the stress, the effect of stress was not incorporated in the definition of Young's modulus as this effect was negligible for the alloys used in the experiments back then. Unlike earlier work [1] where the ΔE effect was defined at different constant stresses (σ), Lee [6] defined the ΔE effect as $(E_S - E_a)$ in the limit of $\sigma \rightarrow 0$ and stated based on this definition that the ΔE effect should be always positive irrespective of the sign of magnetostriction. A later work [7] used an internal stress distribution theory to model the ΔE effect as a function of stress in iron-germanium alloys.

With the discovery of rare-earth-iron compounds which exhibited giant magnetostriction, a normalized ΔE effect given by the expression $(E_S - E_a)/E_a$, was used [8] to show around 90 % change in modulus in $TbFe_2$ between its demagnetized and saturated states which was significantly higher than that of iron (0.4 %) and nickel (6-18 %) [9]. These studies used acoustic as well as static stress-strain measurement and reported 17 % difference in the hard modulus measured by these two techniques. The discrepancy between the two measurement techniques was attributed to domain reorientation even at 7 MHz. In spite of this reported discrepancy, acoustic measurements were further used [10] to show 144 % ΔE effect in Terfenol-D where the soft modulus was estimated from low resonance frequency and the hard modulus was estimated from high resonance frequency at demagnetized and magnetized conditions respectively. A different work [9] reported 161 % ΔE effect

in Terfenol-D using acoustic measurement. The nature of measurement in this work prevented the analysis of the effect of stress. Furthermore, it was shown that the Young's modulus monotonically increased as a function of the applied magnetic field. From earlier discussion and from the work of Honda [1], we know that the modulus at magnetic saturation (E_S) should be a constant. Evidence of a monotonically increasing modulus with increasing magnetic field is indicative of the challenges in using these measurement techniques to determine the saturation modulus in materials such as Terfenol-D, with magnetic easy axes aligned along [111] instead of the direction of the applied field (i.e. [112]).

The variation of Young's modulus with applied magnetic field was reported [11] for Metglas using dynamic measurement. It was shown in this work that the Young's modulus initially decreases with increasing magnetic field till it reaches a minimum at some non-zero magnetic field beyond which it increases with increasing magnetic field. Neither the effect of stress nor the effect of high magnetic field which should help in the observation of E_S was discussed. Nevertheless, this work [11] confirmed that the largest change in modulus is not observed between demagnetized and saturated conditions. A later work [12] measured the Young's modulus of Terfenol-D as a function of stress at different applied magnetic fields using static stress-strain measurement under compressive loads. It was shown [12] that for any given applied magnetic field, the Young's modulus initially decreases with increasing compressive stress till it reaches a minimum at some non-zero stress beyond which it increases with increasing compressive stress until the material is saturated. Trends in variation of Young's modulus observed by Anderson [11] in Metglas for varying magnetic field and by Savage [12] in Terfenol-D for varying stress were similar indicating the lowest Young's modulus in a magnetostrictive material is obtained at non-zero operating stress and magnetic field conditions.

Another quantity of interest studied by several researchers [13-15] is the Young's modulus at constant magnetic induction (E_B). This quantity can be measured from the stress-strain curve of a material provided the magnetic induction is kept constant throughout the stress cycle by appropriately adjusting the magnetic field. For all non-zero magnetic fields, E_S and E^B are equal to each other (and are constant in value) only beyond saturation. If a stress is applied in the absence of a magnetic field, then the magnetic moments could rotate while maintaining a zero magnetic induction, producing a non-zero magnetoelastic strain and hence E_S and E_B are not equal unless all moments are aligned antiparallely. As expected from the theory, both E_H and E_B were shown [13-15] to vary in rare-earth compounds based on the stress and magnetization states of the material.

Kim et al. [16] showed experimental variation in Young's modulus as a function of magnetic field at different stress levels and also as a function of tensile stress at different applied magnetic fields in amorphous magnetostrictive ribbons. A one dimensional energy-based model [16] using the internal stress distribution theory [7] showed good correlation with the experimental modulus. Kellogg and Flatau [2, 17] showed the effect of magnetic field on Young's modulus of Terfenol-D at different pre-stresses using dynamic measurement [2] and the effect of stress on Young's modulus of Terfenol-D at different bias magnetic fields using quasi-static stress-strain measurement [17]. In order to get useful information for design of tunable mechanical resonators in which the ΔE effect was used to selectively, electrically adjust resonance of the device [2, 17], the term $\Delta E_{H_2H_1} = (E_{H_2} - E_{H_1})/E_{H_2}$ was introduced to describe the change in Young's modulus about a given operating stress as the applied magnetic field changed from H_1 to H_2 . Interestingly, this definition introduced a possibility of having positive and negative value of $\Delta E_{H_2H_1}$ at different operating regimes as shown earlier by Honda [1], unlike the ΔE effect defined by Lee [6].

The earliest measurement of magnetic field-dependent stiffness constants c_{44} and c' [$= (c_{11} - c_{12})/2$] in iron-gallium (Galfenol) alloys was reported by Petculescu et al. [18] using resonance ultrasound spectroscopy. They measured $\Delta c'$ and Δc_{44} of both water quenched and furnace cooled single crystal Galfenol with 12-33.3 atomic % gallium under zero and 15 kOe (1193 kA/m) of applied magnetic fields. Kellogg et al. [19] and Atulasimha et al. [20] studied the effect of varying compressive stress at constant current to a solenoid surrounding a sample and constant magnetic fields on the Young's modulus of water quenched and furnace cooled $Fe_{81}Ga_{19}$ respectively. Atulasimha et al. [20] also showed that variation of stress can change the permeability in the

magnetostrictive material and hence estimates of E_H based on use of a constant current for producing a magnetic field can be significantly different from the desired modulus for a constant applied magnetic field, E_H .

The ability to quantify the relative magnitude of variability in elastic modulus in a form that can readily be used for device design, e.g. in tunable resonators and for real-time impedance matching, motivates the introduction of the “bounded ΔE ” function given in Eq. (2), $\Delta E(\sigma, H)$, which limits variability of modulus to extreme values of between 0 and 100 %. In this equation, the change in modulus between saturation and an operating condition defined by the stress and magnetic field, is normalized with respect to the constant saturation modulus instead of a variable soft modulus (instead of with respect to the stress and field dependent soft modulus). As a result, the $\Delta E(\sigma, H)$ will always be positive and will have lower and upper bounds of 0 and 100 % corresponding to the perfectly saturated state [$E(\sigma, H) = E_S$] of the material and a perfectly dissociated state [$E(\sigma, H) = 0$] of the material respectively. It was deemed useful to avoid the use of the demagnetized modulus (E_a) as its value can vary based on the sample history as there is no unique demagnetized state for a material.

$$\Delta E(\sigma, H) = \frac{E_S - E(\sigma, H)}{E_S} \quad (2)$$

This paper presents experimental values of Young’s modulus of single crystal iron-gallium (Galfenol) alloys having 16 and 19 atomic percent gallium which were measured as a function of stress and magnetic field. A feedback controller was used in the experiment to maintain constant internal magnetic field in the samples. It is also shown that an energy-based non-linear constitutive model can be used to predict the Young’s modulus as a continuous function of stress and magnetic field in the magnetostrictive material.

2. MAGNETOMECHANICAL CHARACTERIZATION

This section describes the quasi-static stress-strain characterization performed on the $\text{Fe}_{84}\text{Ga}_{16}$ and $\text{Fe}_{81}\text{Ga}_{19}$ rod-shaped samples under different constant bias magnetic fields. The samples were prepared at Materials Preparation Center, Ames [21]. The $\text{Fe}_{84}\text{Ga}_{16}$ sample was 25-mm long and 6.25-mm in diameter and the $\text{Fe}_{81}\text{Ga}_{19}$ sample was 29.21-mm long and 6.21-mm in diameter. Both the samples used in this study can be considered to be in the “furnace cooled” state and all measurements were made along the [100] crystallographic direction of the samples.

An in-house built transducer [19] was used to characterize the sample. The magnetomechanical characterization involved measurement of the strain of the sample under quasi-static compressive stress that varied from zero to 120 MPa and back to zero at a linear ramp rate of 2 MPa/s while the sample was subjected to different DC bias magnetic fields from 0 to 71 kA/m. The compressive stress cycle was applied using a hydraulic MTS 810 universal testing machine in feedback force-control mode. The compressive force was measured using a load cell. The strain in the sample was measured by two resistive strain gages attached in a quarter bridge configuration on diametrically opposite sides of the rod at mid-length to counter the effect of any bending moment. A linear Hall-effect sensor placed parallel to the sample measured the magnetic field. A feedback controller [22] was used to measure the response from the Hall-effect sensor and adjust the current in the drive coil to maintain a constant magnetic bias field in the sample throughout the stress cycle. Fig. 1 shows the block diagram of the feedback control system which was used to obtain the desired field.

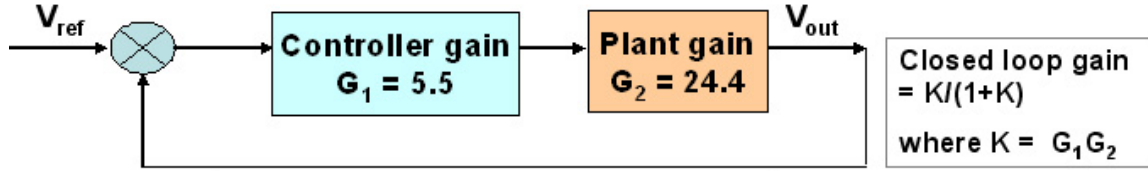


Figure 1. Block diagram of feedback controller system used to maintain a constant magnetic field in the sample during a quasi-static stress cycle.

The test sequence comprised of demagnetizing the sample followed by applying the DC bias magnetic field and cycling the stress. The demagnetization sequence lasted over 167 cycles using a 1 Hz sinusoidal field which underwent a 5 % geometric decay every 1.5 cycles from an initial amplitude of 97 kA/m. The data was collected using a computer-controlled system at 50 scans per second.

3. MAGNETOMECHANICAL MODEL

This section describes an energy-based non-linear magnetomechanical model which was used to obtain the magnetoelastic strain as a function of stress and magnetic field. This approach was originally used by Armstrong to model the magnetostriction in Terfenol-D [23] and was later adapted to both model the actuator and predict the sensor responses of single crystal and polycrystalline Galfenol subjected to axial stress [24]. In the current work, this modeling approach is used to predict the magnetoelastic strain of a single crystal rod along its [100] longitudinal axis. The model uses the saturation magnetization (M_s), the magnetostrictive constant (λ_{100}) and the 4th and 6th order magnetocrystalline anisotropy constants (K_1 and K_2) to calculate the Zeeman, stress-induced anisotropy and magnetocrystalline anisotropy energies per unit volume due to a magnetic field (H) and stress (σ) applied along the [100] direction as shown in Eqs. (3), (4) and (5) respectively.

$$E_H = -\mu_o M_s H \alpha_1 \quad (3)$$

$$E_\sigma = -\frac{3}{2} \lambda_{100} \sigma \alpha_1^2 \quad (4)$$

$$E_{an} = K_1 (\alpha_1^2 \alpha_2^2 + \alpha_2^2 \alpha_3^2 + \alpha_3^2 \alpha_1^2) + K_2 (\alpha_1^2 \alpha_2^2 \alpha_3^2) \quad (5)$$

$$E_{TOT}(\varphi, \theta) = E_H + \gamma_\sigma E_\sigma + E_{an} \quad (6)$$

The total energy (E_{TOT}) of the system corresponding to different orientations of the local magnetization vectors can be expressed in terms of their direction cosines ($\alpha_1, \alpha_2, \alpha_3$) as shown in Eq. (6). The direction cosines can be expressed in terms of the azimuthal angle (φ) and the polar angle (θ) such that $\alpha_1 = \sin \theta \cos \varphi$, $\alpha_2 = \sin \theta \sin \varphi$ and $\alpha_3 = \cos \theta$. The empirical parameter (γ_σ) was used to accommodate the need for a linear correction to the contribution of the stress-induced anisotropy energy to improve the model fit of experimental data [25]. The total energy in this model is formulated with stress induced anisotropy energy and appears to omit the magnetoelastic, elastic, and mechanical work energies, however, recent work [26] shows the equivalence of these terms.

Assuming the sample is comprised of a large number of equivalent magnetization units, each of them is likely to have a particular orientation of magnetization with a probability that depends on the energy corresponding to that orientation. The defocusing of the local magnetization about the average magnetization direction is modeled [23] by assuming that the probability of the magnetization vector orienting along a particular direction is proportional to the inverse exponential of the energy (E_{TOT}) divided by an empirical factor Ω that accounts for the local fluctuations. Since magnetostriction also depends on the orientation of the magnetization vector, the same hypothesis

can be extended to calculate magnetostriction along [100] using Eq. (7). The total strain can be calculated using Eq. (1).

$$\lambda(\sigma, H) = \frac{\sum_{\varphi=0}^{2\pi} \sum_{\theta=0}^{\pi} \frac{3}{2} \lambda_{100} \left(\alpha_1^2 - \frac{1}{3} \right) |\sin \theta| \Delta \theta \Delta \varphi e^{\frac{-E_{TOT}}{\Omega}}}{\sum_{\varphi=0}^{2\pi} \sum_{\theta=0}^{\pi} |\sin \theta| \Delta \theta \Delta \varphi e^{\frac{-E_{TOT}}{\Omega}}} \quad (7)$$

The model parameters used for the two different samples in this work are shown in Table 1. Model parameters such as magnetostrictive constant (λ_{100}) and saturation Young's modulus (E_S) were obtained from the experiment described in section 2. The method for obtaining other model parameters such as M_s , K_1 , K_2 , γ_σ and Ω is described in other works [27, 28]. A detailed study of the effect of the model parameters on the model prediction can be found in Atulasimha et al. [25]. An optimum value of $\Delta\varphi = \Delta\theta = 5^\circ$ was used for all cases to get converged solutions within reasonable computation time.

Table 1. Model parameters used in energy-based model.

Parameters	M_s [kA/m]	λ_{100} [$\mu\epsilon$]	K_1 [kJ/m ³]	K_2 [kJ/m ³]	γ_σ	Ω [J/m ³]	E_S [GPa]
Fe₈₄Ga₁₆	1456	165	13	-90	0.875	600	76
Fe₈₁Ga₁₉	1321	212	17.5	0	0.9	707	59

4. RESULTS AND DISCUSSION

This section shows the strain-stress relationship in Fe₈₄Ga₁₆ and Fe₈₁Ga₁₉ under different constant magnetic fields. For all cases discussed in this work, the stress and magnetic field were applied along the [100] crystallographic direction of the sample and the corresponding strain was measured or predicted with the model along the same direction. The Young's modulus was obtained as a function of stress and magnetic field from measured values of the stress-strain gradient for a given constant magnetic field as well as from predictions obtained by using the energy-based model. The common trends as well as differences exhibited by the two samples are discussed with respect to the different energy terms introduced in Eqs. (3) – (5).

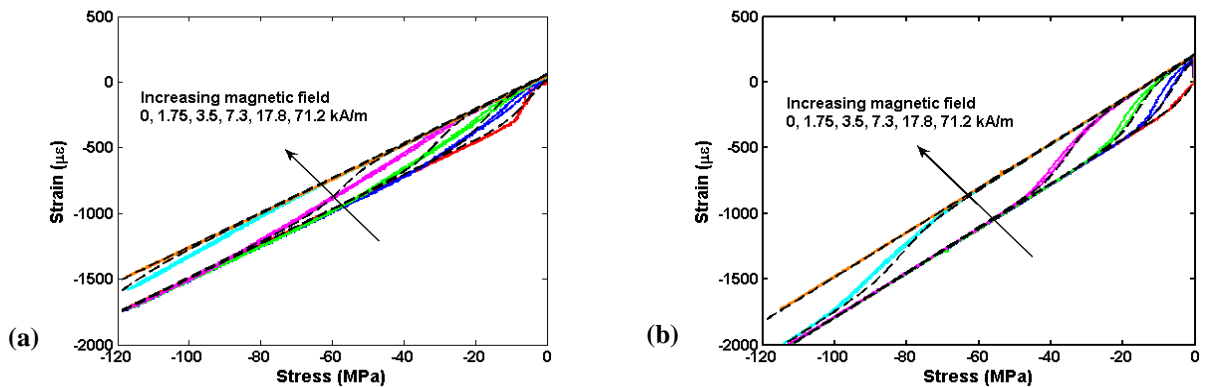


Figure 2. Energy-based model prediction (black dashed lines) and experimental (colored lines) strain (ϵ) vs. compressive stress (σ) at DC bias magnetic fields (H) of 0-71.2 kA/m for (a) Fe₈₄Ga₁₆ and (b) Fe₈₁Ga₁₉.

Fig. 2 shows the strain in Fe₈₄Ga₁₆ and Fe₈₁Ga₁₉ as a function of the quasi-static compressive

stress at different constant magnetic fields in the samples. At zero bias field and zero stress, no strain is observed in the samples. On increasing the compressive stress from zero, a non-linear elastic region is observed, which corresponds to additional magnetoelastic strain due to magnetic moment rotation, superimposed on the elastic strain. Beyond a critical compressive stress (~ 20 MPa), which is required to overcome the magnetocrystalline anisotropy, all the magnetic moments align along the equilibrium [010] or [001] direction and hence a linear ε - σ curve is observed. It should be noted that the magnetocrystalline anisotropy in Galfenol alloys with 16 and 19 atomic % gallium favors the alignment of the magnetic moments along the six equivalent $\langle 100 \rangle$ crystallographic directions in the absence of any external stress and magnetic field.

On application of a bias field, the samples exhibit magnetoelastic strain even at zero stress due to the magnetic moment rotation from [010] or [001] to [100] produced by the magnetic field. On increasing the compressive stress from zero, a linear ε - σ curve is seen until the stress-induced anisotropy overcomes the Zeeman and magnetocrystalline anisotropy energies and the magnetic moments start to rotate away from [100]. The magnetic moment rotation is exhibited by a non-linear region in the ε - σ curve, which becomes linear once again at high stresses when all the magnetic moments have rotated to either of the two [100] directions. The higher the bias field, the higher is the energy barrier that has to be overcome by the compressive stress in order to rotate the magnetic moments and hence the non-linearity in the ε - σ curves gets shifted towards higher compressive stresses at higher bias fields. The stress range used for the experiment was not sufficient to overcome the Zeeman energy due to 71 kA/m and hence the magnetic moments in the sample remain aligned along [100] throughout the stress cycle at this bias field.

The model predictions obtained using the energy-based approach are superimposed on the experimental results in Fig. 2. The Young's modulus was calculated from the experimental ε - σ curves using a moving average scheme. This method reduced the large error that can arise if numerical differentiation is performed on experimental data which is not smooth. A window of 4 MPa (~ 30 data points) was chosen and a straight line was fitted to all the data points lying inside this window. The inverse of the slope of the line gave the Young's modulus at the mean value of the stress range of that window. The window was moved across the entire range of data to obtain the Young's modulus as a function of stress at different DC bias magnetic fields.

In order to obtain the Young's modulus as a continuous function of stress and magnetic field, the energy-based model was used to generate ε - σ curves for compressive stresses ranging from -150 to 50 MPa at an interval of 1 MPa and magnetic fields ranging from 0 to 100 kA/m at an interval of 0.1 kA/m. The first derivative of these curves obtained by numerical differentiation as shown in Eq. (8) gave the Young's modulus as a function of magnetic field and stress in the sample.

$$E_{ij}(\sigma_i, H_j) = \left. \frac{\sigma_{i+1} - \sigma_{i-1}}{\varepsilon_{i+1} - \varepsilon_{i-1}} \right|_{H_j} \quad (8)$$

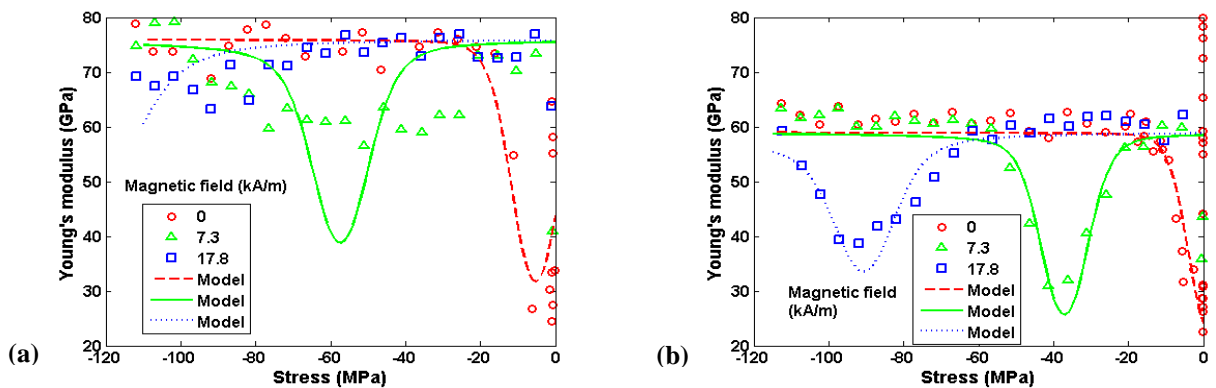


Figure 3. Energy-based model prediction (lines) and experimental (markers) Young's modulus (E) vs. compressive stress (σ) at DC bias magnetic fields (H) of 0, 7.3 and 17.8 kA/m for (a) $\text{Fe}_{84}\text{Ga}_{16}$ and (b) $\text{Fe}_{81}\text{Ga}_{19}$.

Fig. 3 shows that the model predictions capture the trend in the Young's modulus with varying stress and magnetic field quite well. However the model appears to over-predict or under-predict the modulus in certain regions. Error between the experimentally obtained values and model predictions can be traced back to the fact that the model provides a good fit of the ϵ - σ curves on an average sense and not at all points on these curves. Any small deviation of the model from the experimental curves would be amplified during the numerical differentiation required to obtain the material properties. Furthermore, the use of the moving average scheme to estimate the modulus and choosing a window of 4 MPa in this scheme does not eliminate errors associated with inaccuracies in the energy model but rather contributes to reducing noise estimate that arises due to numerical differentiation.

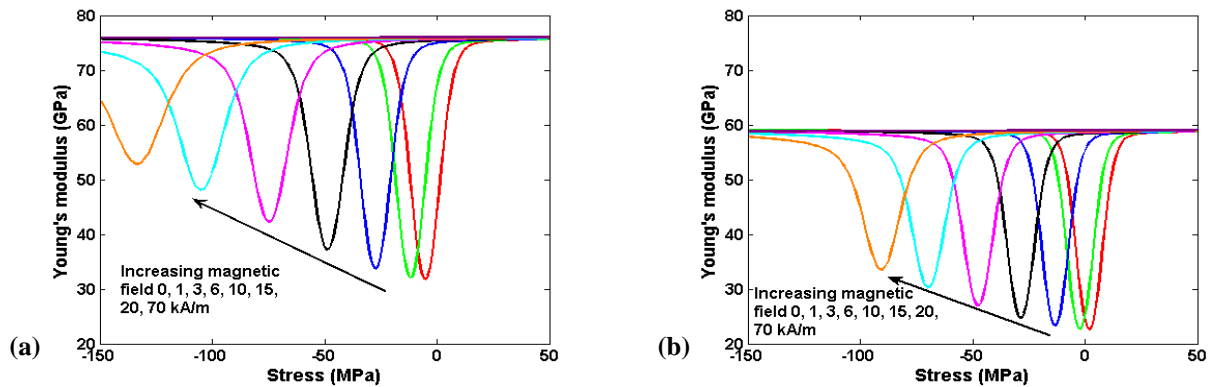


Figure 4. Energy-based model prediction of Young's modulus (E) vs. stress (σ) at magnetic fields (H) of 0-70 kA/m for (a) $\text{Fe}_{84}\text{Ga}_{16}$ and (b) $\text{Fe}_{81}\text{Ga}_{19}$. For both the samples, no ΔE effect was observed for $H = 70$ kA/m in this stress range.

Fig. 4 shows the model simulation of Young's modulus as a function of compressive and tensile stresses at different constant magnetic fields. If the bias field is kept constant and a compressive stress is applied, the Young's modulus initially decreases due to additional magnetoelastic strain produced by magnetic moment rotation till it reaches a minimum value. With further increase in the compressive stress, E increases and asymptotes to a value corresponding to the saturation Young's modulus (E_S) and a state in which the magnetic moments are oriented close to [010] or [001]. Application of a tensile stress at a constant magnetic field, helps align magnetic moments along the [100] direction. Hence even a small tensile stress rapidly increases the Young's modulus to its saturation value and a state with magnetic moments aligned along the [100] direction. Also, it should be noted that the ΔE effect can be observed at any magnetic field provided the compressive stress applied is high enough to overcome the Zeeman and magnetocrystalline anisotropy energies.

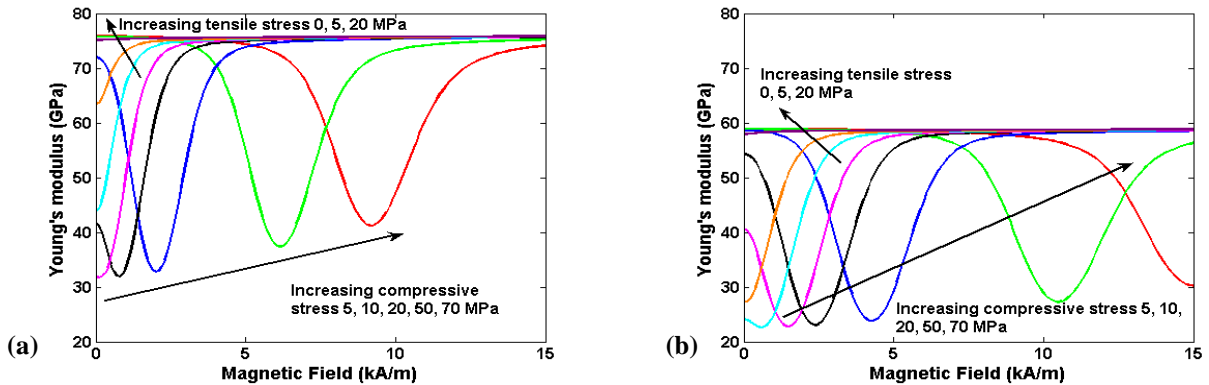


Figure 5. Energy-based model prediction of Young's modulus (E) vs. magnetic field (H) at pre-stresses (σ) of +20 to -70 MPa for (a) $\text{Fe}_{84}\text{Ga}_{16}$ and (b) $\text{Fe}_{81}\text{Ga}_{19}$. For both the samples, no ΔE effect is nearly zero for a tensile stress of 20 MPa.

Fig. 5 shows the model simulation of Young's modulus as a function of magnetic field at different constant tensile and compressive stresses. Under constant value of compressive stresses, increasing the magnetic field will cause the modulus to decrease until it reaches a minimum value. The large drop in modulus occurs once the Zeeman energy introduced by the applied field is high enough to overcome the stress-induced and magnetocrystalline anisotropy energies. Once the minimum value is reached, further increases in the magnetic field cause the modulus to increase until it reaches the saturation value (E_S) at a magnetic field which is high enough to align all the magnetic moments along [100]. If the stress is tensile, increasing the magnetic field helps align the magnetic moments along [100] and therefore the modulus increases till it reaches E_S . It should be noted that the ΔE effect cannot be observed at any magnetic field if the initial tensile stress applied is high enough to saturate the material, as shown in Fig. 5 for the case of 20 MPa tensile stress. In a sample which has been saturated by applying a high enough tensile pre-stress, an increasing magnetic field simply flips the magnetic moments from $[\bar{1}00]$ to [100] as soon as the field is sufficient to overcome the magnetocrystalline anisotropy. Such a 180° rotation of magnetic moments does not contribute to ΔE effect as explained in details later.

An important feature that needs to be discussed is the trend in the magnitude of the minima in modulus when either stress or magnetic field is kept constant while the other is varied. Both Figs. 4 and 5 show that the lowest possible modulus is obtained at small values of magnetic field and small values of compressive stress. Fig. 4 shows that as the bias magnetic field is increased, not only do the minima in modulus occur at higher compressive stresses but also the magnitude of the minimum modulus decreases with increasing bias field. Fig. 5 shows that as the pre-stress changes from tensile to compressive, definite minima in modulus start to appear. As the compressive pre-stress is increased, not only do the minima in modulus occur at higher magnetic fields but also the magnitude of the minimum modulus decreases with increasing compressive pre-stress.

An explanation of this trend can be given using the energy plots shown in Fig. 6. The variation in Young's modulus depends on the volume fraction of magnetic moments available which can undergo non- 180° rotation. Hence the extent of variation in Young's modulus depends on the bias magnetic field and/or pre-stress, both of which influence both the volume fraction of magnetic moments which are available for non- 180° rotation and the energy barrier that needs to be overcome by the stress-induced anisotropy or Zeeman energy respectively in order to rotate the magnetic moments from the direction of one energy minima to another. The volume fraction of magnetic moments residing in an energy well is proportional to the depth of the energy well. The minima in modulus denote the operating condition such that a small perturbation in either the magnetic field or stress results in the rotation of maximum volume fraction of magnetic moments. Such a condition requires availability of shallow energy wells at non- 180° intervals which correspond to low stresses and magnetic fields as represented in Fig. 6(a). If the stress-induced anisotropy is significantly higher than the Zeeman energy then there is no possibility of non- 180° rotation as there are only two energy wells separated by a 180° interval as denoted by $\sigma = \pm 50$ MPa curves in Fig. 6(a). The saturation modulus is obtained under such conditions. Conversely, if the Zeeman energy is significantly higher than the stress-induced anisotropy, there cannot be any non- 180° rotation as energy wells occur at 0° and 180° , as for the 50 MPa tensile stress case in Fig. 6(b) or only at 0° , as for all other cases in Fig. 6(b). The saturation modulus can also be obtained under all of the conditions shown in Fig. 6(b). In general, the higher the bias magnetic field or pre-stress, the lower the volume fraction of magnetic moments that are available for non- 180° rotation and hence the smaller the minima in Young's modulus.

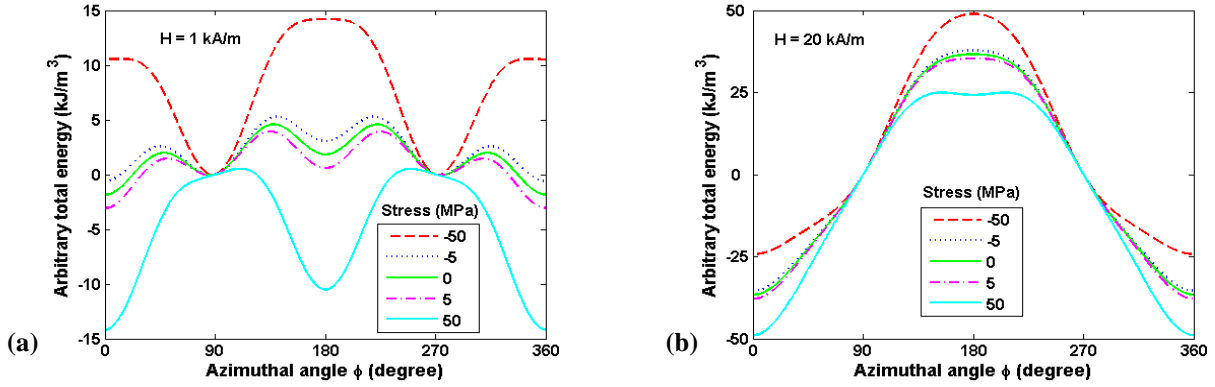


Figure 6. Arbitrary total energy (E_{TOT}) vs. azimuthal angle (ϕ) of magnetization direction at constant magnetic fields of (a) 1 kA/m and (b) 20 kA/m for stresses ranging from -50 to 50 MPa. The energy map is plotted at a polar angle (θ) of 90° , i.e. in the azimuthal plane.

In both samples, the lowest possible modulus, $E(\sigma, H)_{\min}$ was observed at small compressive stresses ($0 < \sigma < 20$ MPa) and low magnetic fields ($0 < H < 5$ kA/m). The maximum $\Delta E(\sigma, H)$ experimentally observed in $\text{Fe}_{84}\text{Ga}_{16}$ and $\text{Fe}_{81}\text{Ga}_{19}$ were 54 % and 63 % respectively. The model prediction estimated the maximum $\Delta E(\sigma, H)$ in $\text{Fe}_{84}\text{Ga}_{16}$ and $\text{Fe}_{81}\text{Ga}_{19}$ as 58 % and 63 % respectively. The model prediction of the value of maximum $\Delta E(\sigma, H)$ as well as the operating point where it is observed agree well with the experimental results. The significant results are summarized in Table 2.

Table 2. Summary of variable Young's modulus in $\text{Fe}_{84}\text{Ga}_{16}$ and $\text{Fe}_{81}\text{Ga}_{19}$.

Sample	E_s	E_a	Normalized ΔE effect (%)	Minimum $E(\sigma, H)$	$\Delta E(\sigma, H)_{\max}$ (%)
	[GPa]	[GPa]	$\Delta E = (E_s - E_a)/E_a$ [8]	[GPa]	$\Delta E(\sigma, H)_{\max} = (E_s - E(\sigma, H)_{\min})/E_s$
$\text{Fe}_{84}\text{Ga}_{16}$	76	44	73	32	58
$\text{Fe}_{81}\text{Ga}_{19}$	59	24	146	22	63

Although the general trend in the variation of E with respect to σ and H are same in both the samples, specific differences at any given operating point can be observed due to the difference in material properties between the two compositions. For example, at $H = 20$ kA/m and $\sigma = -150$ MPa, the Young's modulus in $\text{Fe}_{84}\text{Ga}_{16}$ does not reach E_s while the same in $\text{Fe}_{81}\text{Ga}_{19}$ almost reaches E_s . This is due to the fact that $\text{Fe}_{84}\text{Ga}_{16}$ has a higher M_s and lower λ_{100} than $\text{Fe}_{81}\text{Ga}_{19}$ and hence for a given combination of stress and magnetic field, the relative difference between the stress induced anisotropy and Zeeman energies is more in $\text{Fe}_{84}\text{Ga}_{16}$ than in $\text{Fe}_{81}\text{Ga}_{19}$. This also translates to the fact that for a given bias field, a higher compressive stress is required to saturate $\text{Fe}_{84}\text{Ga}_{16}$ than $\text{Fe}_{81}\text{Ga}_{19}$.

5. CONCLUSIONS

The effect of stress and magnetic field on Young's modulus in magnetostrictive single crystal $\text{Fe}_{84}\text{Ga}_{16}$ and $\text{Fe}_{81}\text{Ga}_{19}$ was investigated using experimental stress-strain characterization under different constant magnetic fields. A feedback control loop was employed to maintain constant magnetic field during the entire stress cycle used for the characterization to ensure accurate estimation of Young's modulus. An energy-based non-linear constitutive magnetomechanical model was used to predict the Young's modulus as a continuous function of stress and magnetic field.

Most existing work on the ΔE effect uses a value obtained between zero and saturating magnetic fields and as stress tends to zero. The results of this work showed that for both the compositions, the minimum value of Young's modulus was observed for compressive stresses lower than 20 MPa and below magnetic field of 5 kA/m but not at $H = 0$ and $\sigma \rightarrow 0$. A survey of literature on

the ΔE effect in magnetostrictive materials was performed and a new parameter, the bounded $\Delta E(\sigma, H)$, was introduced to include the effect of both stress and magnetic field. The normalization of the change in modulus in the new parameter $\Delta E(\sigma, H)$ was done with respect to the Young's modulus at magnetic saturation so as to provide 100 and 0 as upper and lower bounds, respectively, irrespective of the material being studied. Both experimental study and model prediction suggested $\Delta E(\sigma, H)$ as high as 60 % in magnetostrictive single crystal Galfenol. It was shown that the change in modulus can be produced by varying both magnetic field and stress in a magnetostrictive material and hence they can be used in design of smart material applications such as tunable resonators, active vibration control devices, acoustic wave guides and mechanical or magnetic field sensors.

ACKNOWLEDGEMENTS

This work was supported by ONR MURI Grant No. N000140610530.

REFERENCES

1. Honda, K. and T. Terada, "On the change of elastic constants of ferromagnetic substances by magnetization.," *Philosophical Magazine*, Vol. 13, pp. 36-83, (1907).
2. Kellogg, R. and A. Flatau, "Wide Band Tunable Mechanical Resonator Employing the ΔE Effect of Terfenol-D," *Journal of Intelligent Material Systems and Structures*, Vol. 15(5), pp. 355-368, (2004).
3. Engdahl, G., *Handbook of Giant Magnetostrictive Materials*, San Diego: Academic Press, (2000).
4. Forster, V.F. and W. Koster, "Uber die Abhangigkeit des Elastizitatsmoduls und der Dampfung Transversal schwingender Metallstabe von der Amplitude," *Die Naturwissenschaften*, Vol. 25(26-27), pp. 436-439, (1937).
5. Becker, R. and W. Doring, *Ferromagnetismus*, Berlin: Verlag. Julius Springer, (1939).
6. Lee, E.W., "Magnetostriction and Magnetomechanical Effects," *Reports on Progress in Physics*, Vol. 18(1), pp. 184-229, (1955).
7. Smith, G.W. and J.R. Birchak, "Application of Internal-Stress-Distribution Theory to Delta E Effect, Initial Permeability, and Temperature-Dependent Magnetomechanical Damping," *Journal of Applied Physics*, Vol. 41(8), pp. 3315-3321, (1970).
8. Clark, A.E., H.S. Belson, and R.E. Strakna, "Elastic properties of rare-earth-iron compounds," *Journal of Applied Physics*, Vol. 44(6), pp. 2913-2914, (1973).
9. Clark, A.E. and H.T. Savage, "Giant Magnetically Induced Changes in the Elastic Moduli in $Tb_3Dy_7Fe_2$," *IEEE Transactions on Sonics and Ultrasonics*, Vol. 22(1), pp. 50-51, (1975).
10. Savage, H.T., A.E. Clark, and J.M. Powers, "Magnetomechanical coupling and DE effect in highly magnetostrictive rare earth - Fe_2 compounds," *IEEE Transactions on Magnetics*, Vol. 11(5), pp. 1355-1357, (1975).
11. Anderson, P.M., "Magnetomechanical coupling, Delta E effect, and permeability in FeSiB and FeNiMoB alloys," *Journal of Applied Physics*, Vol. 53(11), pp. 8101-8103, (1982).
12. Savage, H.T., A.E. Clark, and D. Pearson, "The stress dependence of the Delta E effect in Terfenol-D (abstract)," *Journal of Applied Physics*, Vol. 64(10), pp. 5426, (1988).
13. Clark, A.E., et al., "Magnetoelastic coupling and Delta E effect in Tb_xDy_{1-x} single crystals," *Journal of Applied Physics*, Vol. 73(10), pp. 6150-6152, (1993).
14. Clark, A.E., et al., "Magnetization, Young's moduli, and magnetostriction of rare-earth--iron eutectic alloys with $R=Tb_{0.6}Dy_{0.4}$," *Journal of Applied Physics*, Vol. 76(10), pp. 7009-7011, (1994).

15. Restorff, J.B., M. Wun-Fogle, and A.E. Clark, "Piezomagnetic properties, saturation magnetostriction, and Delta E effect in DyZn at 77 K," *Journal of Applied Physics*, Vol. 83(11), pp. 7288-7290, (1998).
16. Kim, D.Y., et al., "Stress dependence of Delta E in amorphous ribbon," *Journal of Applied Physics*, Vol. 81(8), pp. 5811-5813, (1997).
17. Kellogg, R. and A.B. Flatau, "Experimental Investigation of Terfenol-D's Elastic Modulus," *Journal of Intelligent Material Systems and Structures*, Vol. 19(5), pp. 583-595, (2008).
18. Petculescu, G., et al., "Magnetic field dependence of galfenol elastic properties," *Journal of Applied Physics*, Vol. 97(10), pp. 10M315, (2005).
19. Kellogg, R.A., et al., "Quasi-static Transduction Characterization of Galfenol," *Journal of Intelligent Material Systems and Structures*, Vol. 16(6), pp. 471-479, (2005).
20. Atulasimha, J., A.B. Flatau, and R.A. Kellogg, "Sensing Behavior of Varied Stoichiometry Single Crystal Fe-Ga," *Journal of Intelligent Material Systems and Structures*, Vol. 17(2), pp. 97-105, (2006).
21. *Single crystal synthesized at the Materials Preparation Center, Ames Laboratory, USDOE. See www.mpc.ameslab.gov.* (2008).
22. Atulasimha, J. and A.B. Flatau, "Experimental Actuation and Sensing Behavior of Single-crystal Iron-Gallium Alloys," *Journal of Intelligent Material Systems and Structures*, doi:10.1177/1045389X07086538, (May 2008).
23. Armstrong, W.D., "Magnetization and magnetostriction processes in $Tb_{0.27-0.30}Dy_{0.73-0.70}Fe_{1.9-2.0}$," *Journal of Applied Physics*, Vol. 81(5), pp. 2321-2326, (1997).
24. Atulasimha, J., A.B. Flatau, and E. Summers, "Characterization and energy-based model of the magnetomechanical behavior of polycrystalline iron-gallium alloys," *Smart Materials and Structures*, Vol. 16(4), pp. 1265-1276, (2007).
25. Atulasimha, J., A.B. Flatau, and J.R. Cullen, "Analysis of the effect of gallium content on the magnetomechanical behavior of single-crystal FeGa alloys using an energy-based model," *Smart Materials and Structures*, Vol. 7(2), pp. 025027, (2008).
26. Mudivarthi, C., et al. "Equivalence of magnetoelastic, elastic, and mechanical work energies with stress-induced anisotropy," in *Behavior and Mechanics of Multifunctional and Composite Materials*, Proceedings of SPIE, San Diego, CA, Vol. 6929, pp. 69291X, (2008).
27. Atulasimha, J., A.B. Flatau, and J.R. Cullen, "Energy-based quasi-static modeling of the actuation and sensing behavior of single-crystal iron-gallium alloys," *Journal of Applied Physics*, Vol. 103(1), pp. 014901, (2008).
28. Datta, S. and A.B. Flatau, "Magnetomechanical coupling factor and energy density of single crystal iron-gallium alloys," in *Behavior and Mechanics of Multifunctional and Composite Materials*, Proceedings of SPIE, San Diego, CA, Vol. 6929, pp. 69291Z, (2008).